

---

# Field Symmetry Theory: A Phenomenological Model for Nuclear Binding Energy with 99.9% Accuracy for Heavy Nuclei

---

[Raheb Ali Mohammed Saleh Aoudh](#) \*

Posted Date: 9 March 2026

doi: 10.20944/preprints202603.0650.v1

Keywords: nuclear binding energy; field symmetry theory; semi-empirical mass formula; Bethe-Weizsäcker formula; liquid drop model; Heisenberg uncertainty principle; renormalization group; Lorentzian correction; AME2020; heavy nuclei; uranium isotopes



Preprints.org is a free multidisciplinary platform providing preprint service that is dedicated to making early versions of research outputs permanently available and citable. Preprints posted at Preprints.org appear in Web of Science, Crossref, Google Scholar, Scilit, Europe PMC.

Copyright: This open access article is published under a [Creative Commons CC BY 4.0 license](#), which permit the free download, distribution, and reuse, provided that the author and preprint are cited in any reuse.

Disclaimer/Publisher's Note: The statements, opinions, and data contained in all publications are solely those of the individual author(s) and contributor(s) and not of MDPI and/or the editor(s). MDPI and/or the editor(s) disclaim responsibility for any injury to people or property resulting from any ideas, methods, instructions, or products referred to in the content.

Article

# Field Symmetry Theory: A Phenomenological Model for Nuclear Binding Energy with 99.9% Accuracy for Heavy Nuclei

Raheb Ali Mohammed Saleh Aoudh

Independent Researcher, Ibb Governorate, Yemen; o.963852963852@gmail.com

## Abstract

We present a phenomenological model for nuclear binding energy, termed Field Symmetry Theory (FST), based on an effective nuclear field derived from the Heisenberg uncertainty relation. The model incorporates volume, Coulomb, symmetry, and pairing terms as physical corrections, with the logarithmic term  $\ln A$  justified through renormalization group arguments. A Lorentzian correction is introduced to account for few-body effects in light nuclei, with a physical justification based on finite-size effects in quantum systems. With only eight adjustable parameters, the model achieves a mean absolute error of 0.0388 MeV per nucleon and  $R^2 = 0.99996$  when compared to 3554 nuclei from the Atomic Mass Evaluation 2020 (AME2020) dataset. The model performs reasonably well for light nuclei ( $A < 8$ : MAE = 1.15 MeV/n, accuracy 65.8%) and achieves 99.9% accuracy for heavy nuclei ( $A > 150$ ), with uranium isotopes reaching 99.9% precision. Cross-validation confirms no overfitting (generalization gap  $< 10^{-6}$  MeV/n), and correlation analysis reveals expected interdependencies among base parameters while confirming the stability of correction parameters. The complete computational code is provided as supplementary material accompanying this manuscript.

**Keywords:** nuclear binding energy; field symmetry theory; semi-empirical mass formula; Bethe-Weizsäcker formula; liquid drop model; Heisenberg uncertainty principle; renormalization group; Lorentzian correction; AME2020; heavy nuclei; uranium isotopes

## 1. Introduction

The nuclear binding energy has been a central topic in nuclear physics since the discovery of the atomic nucleus. The semi-empirical mass formula, also known as the Bethe-Weizsäcker formula [2,3], provides a macroscopic description based on the liquid drop analogy, incorporating volume, surface, Coulomb, symmetry, and pairing terms. Despite its simplicity, this model has limited accuracy, typically with errors on the order of 1-2 MeV per nucleon.

More sophisticated approaches have been developed, including the Finite Range Droplet Model (FRDM) [4,5] and Skyrme-Hartree-Fock models [6,7], which achieve higher accuracy at the cost of numerous parameters (typically 15-30) and computational complexity. The Duflo-Zuker model [8] represents a benchmark in precision with 28-40 parameters. Recent evaluations [12,13] report RMS deviations of 0.56-0.78 MeV for these models depending on the dataset.

The collective model of Bohr and Mottelson [9–11] has been instrumental in understanding nuclear structure through collective degrees of freedom. In this work, we draw inspiration from this framework to develop a phenomenological field theory for nuclear binding. The model treats the nucleus as a collective excitation of an underlying nuclear field, with physical effects treated as corrections. With only eight adjustable parameters, the model achieves competitive accuracy across the entire nuclear chart, reaching 99.9% accuracy for heavy nuclei ( $A > 150$ ). The model's performance is evaluated through extensive statistical analysis, including cross-validation, sensitivity analysis, correlation analysis, and outlier detection. All computational codes are made available as supplementary material to ensure full reproducibility.

## 2. Theoretical Framework

### 2.1. Derivation of the Field Term

Consider a nucleon confined within a nuclear volume of radius  $R$ . From the Heisenberg uncertainty principle:

$$\Delta p \cdot \Delta x \sim \hbar \quad (1)$$

the characteristic momentum scale is  $p \sim \hbar/R$ . The corresponding energy scale, in the non-relativistic limit appropriate for nucleons in a nucleus, is  $E \sim p^2/2m \sim \hbar^2/(2mR^2)$ . For a system of  $A$  nucleons, if we assume approximate additivity of single-particle energies, the total energy scales as  $A \cdot \hbar^2/(2mR^2)$ . Using the empirical radius  $R = r_0 A^{1/3}$  with  $r_0 \approx 1.25$  fm, this yields an  $A^{1/3}$  scaling, which does not match the observed  $A^{2/3}$  scaling of the surface term.

However, if we consider collective degrees of freedom rather than single-particle ones, the relevant energy scale is  $\hbar c/R$ , and the number of collective modes scales with the surface area  $A^{2/3}$ . This leads to:

$$E_{\text{field}} = \beta_1 C_0 A^{2/3} \quad (2)$$

where  $C_0 = \hbar c/r_0 = 157.8616$  MeV is the fundamental energy constant and  $\beta_1$  is a dimensionless parameter to be determined from data.

### 2.2. Logarithmic Correction

The logarithmic term  $\ln A$  emerges from the renormalization group running of the effective coupling constant. In effective field theory, the coupling constant depends on the energy scale  $\mu$  according to:

$$\frac{dg}{d \ln \mu} = \beta(g) = b_0 g^3 + \mathcal{O}(g^5) \quad (3)$$

For a nuclear system of size  $R$ , the relevant scale is  $\mu \sim 1/R \sim 1/(r_0 A^{1/3})$ . Integrating and expanding to first order yields  $g(A) \approx g_0 + \gamma \ln A$ . Multiplying by the geometric scaling  $A^{2/3}$  gives:

$$E_{\text{field}} = \beta_1 C_0 A^{2/3} + \beta_{\log} C_0 A^{2/3} \ln A \quad (4)$$

This represents the energy contribution from scale-dependent interactions beyond the mean-field approximation.

### 2.3. Physical Corrections

The field terms alone cannot fully describe nuclear binding. Several physical effects must be incorporated:

- **Volume term:**  $E_{\text{vol}} = a_v A$ , representing the bulk energy of nuclear matter.
- **Coulomb term:**  $E_{\text{Coulomb}} = -a_c Z^2/A^{1/3}$ , accounting for electrostatic repulsion between protons.
- **Symmetry term:**  $E_{\text{sym}} = -a_s (N - Z)^2/A$ , favoring equal numbers of protons and neutrons.
- **Pairing term:**  $E_{\text{pair}} = a_p \delta/\sqrt{A}$ , where  $\delta = +1$  for even-even nuclei,  $-1$  for odd-odd nuclei, and  $0$  otherwise.

### 2.4. Lorentzian Correction for Light Nuclei: Physical Justification

For light nuclei ( $A < 20$ ), few-body effects become significant and the collective field approximation breaks down. We introduce a phenomenological correction that decays with mass number. The choice of a Lorentzian (Cauchy) form,

$$E_{\text{corr}} = C_{\text{corr}} \cdot \frac{1}{1 + (A/A_c)^2} \cdot A \quad (5)$$

is motivated by several physical considerations:

- **Finite-size effects in quantum systems:** In a finite system of size  $R \propto A^{1/3}$ , the overlap of surface effects decays as  $1/(1 + (r/R)^2)$  in momentum space, characteristic of a Lorentzian distribution. This form emerges naturally from the Fourier transform of an exponentially decaying density profile [10].
- **Breit-Wigner resonance shape:** The Lorentzian is the natural line shape for resonances in quantum mechanics. Light nuclei often exhibit resonant behavior (e.g.,  $\alpha$ -clustering in  $^{12}\text{C}$ ), and the correction term may be interpreted as an effective parameterization of such resonant contributions.
- **Comparison with alternatives:** While exponential, Gaussian, and Fermi functions were also tested (see Section 3.8), the Lorentzian form provided the best description across the entire light-nuclei region, particularly for the transition region  $8 < A < 20$  where the decay must be neither too sharp (Gaussian) nor too slow (Fermi). The optimized decay constant  $A_c = 3.26$  corresponds to a half-width at half-maximum of  $A_{1/2} = A_c = 3.26$ , indicating that corrections are significant only for  $A < 8$  and become negligible for  $A > 20$ .

### 2.5. Complete FST Model

Combining all terms, the total binding energy is given by:

$$\begin{aligned}
 B(A, Z) = & \beta_1 C_0 A^{2/3} + \beta_{\log} C_0 A^{2/3} \ln A \\
 & + a_v A - a_c \frac{Z^2}{A^{1/3}} - a_a \frac{(N - Z)^2}{A} + a_p \frac{\delta}{\sqrt{A}} \\
 & + C_{\text{corr}} \cdot \frac{1}{1 + (A/A_c)^2} \cdot A
 \end{aligned} \tag{6}$$

### 2.6. Effective Field Coefficient

The combination of the two field terms yields an effective mass-dependent coefficient:

$$\beta_{\text{eff}}(A) = \beta_1 + \beta_{\log} \ln A \tag{7}$$

This quantity measures the importance of collective field effects and should approach zero for heavy nuclei, where the mean-field approximation becomes valid.

## 3. Data and Methodology

### 3.1. Experimental Data

Nuclear binding energies were extracted from the Atomic Mass Evaluation 2020 (AME2020) dataset [1]. Data were filtered according to:

- Mass number  $A \geq 2$
- Binding energy per nucleon between 0.1 and 10 MeV
- Proton number  $Z \leq A$

This yielded 3554 nuclei spanning  $2 \leq A \leq 295$ .

### 3.2. Computational Implementation

The model was implemented in Python 3. The complete computational code, including all routines for data loading, parameter optimization, statistical analysis, and visualization, is provided as supplementary material accompanying this manuscript. This ensures full reproducibility of all results and figures presented in this work.

### 3.3. Parameter Optimization

Parameters were optimized by minimizing the mean absolute error per nucleon:

$$\text{MAE} = \frac{1}{N} \sum_{i=1}^N |B_{\text{exp}}(A_i, Z_i) - B_{\text{calc}}(A_i, Z_i)| \quad (8)$$

using differential evolution [14] to avoid local minima. The stability of the optimization was verified through multiple runs with different initial conditions.

### 3.4. Validation Methods

To assess the model's predictive power and avoid overfitting, we performed:

- 5-fold cross-validation
- Sensitivity analysis with  $\pm 5\%$  parameter variations
- Correlation analysis to quantify parameter interdependencies
- Residual analysis including normality tests and outlier detection
- Exclusion analysis for problematic regions (hydrogen isotopes, very light nuclei)

## 4. Results

### 4.1. Optimized Parameters

**Table 1.** Optimized FST model parameters with uncertainties

Parameter	Value	Uncertainty
$\beta_1$	-0.117749	$\pm 0.0005$
$\beta_{\log}$	0.017084	$\pm 0.0003$
$a_v$ (MeV)	12.872579	$\pm 0.01$
$a_c$ (MeV)	0.631812	$\pm 0.002$
$a_a$ (MeV)	20.458634	$\pm 0.02$
$a_p$ (MeV)	10.359114	$\pm 0.01$
$C_{\text{corr}}$ (MeV)	7.4029	$\pm 0.05$
$A_c$	3.2608	$\pm 0.05$

The volume coefficient  $a_v = 12.87$  MeV is smaller than the typical value of 15-16 MeV in liquid drop models, as part of the volume energy is absorbed into the field terms.

### 4.2. Global Performance

**Table 2.** Global performance metrics

Metric	Value
MAE (total)	2.445 MeV
MAE (per nucleon)	0.0388 MeV
RMSE	3.307 MeV
$R^2$	0.99996
Adjusted $R^2$	0.99996
MAPE	3.74%
AIC	18602.6
BIC	18652.0
Number of nuclei	3554
Number of parameters	8

### 4.3. Mass Range Analysis

**Table 3.** Performance by mass range

Range	A range	Count	MAE (MeV/n)	Accuracy (%)	Correction strength	$\beta_{\text{eff}}$
Extremely Light	2-8	19	1.1486	65.8	0.316	-0.0904
Very Light	8-20	77	0.3267	94.6	0.062	-0.0733
Light	20-50	329	0.1015	98.7	0.010	-0.0572
Medium	50-100	694	0.0359	99.6	0.002	-0.0442
Medium-Heavy	100-150	834	0.0197	99.8	0.001	-0.0354
Heavy	150-200	780	0.0074	99.9	0.0004	-0.0298
Very Heavy	200-300	821	0.0125	99.8	0.0002	-0.0244

The effective coefficient  $\beta_{\text{eff}}(A)$  decreases monotonically with  $A$ , approaching zero for heavy nuclei as expected theoretically. The correction strength becomes negligible for  $A > 50$ . Notably, nuclei in the mass range  $150 < A < 200$  achieve 99.9% accuracy, with a mean absolute error of only 0.0074 MeV/n.

### 4.4. Element Group Analysis

**Table 4.** Performance for selected elements

Element	Z	Isotopes	MAE (MeV/n)	Accuracy (%)
Hydrogen	1	6	2.1099	-42.3
Helium	2	8	0.9960	76.9
Lithium	3	10	0.7005	83.9
Beryllium	4	12	0.4716	90.7
Boron	5	15	0.3723	93.2
Carbon	6	16	0.3285	94.6
Nitrogen	7	16	0.2201	96.6
Oxygen	8	18	0.2280	96.6
Calcium	20	29	0.0527	99.4
Iron	26	32	0.0443	99.5
Tin	50	42	0.0325	99.6
Lead	82	43	0.0203	99.7
Uranium	92	29	0.0070	99.9

The performance improves systematically with increasing  $Z$ , with uranium isotopes reaching 99.9% accuracy.

### 4.5. Pairing Effects Analysis

**Table 5.** Performance by pairing type

Pairing Type	Count	MAE (MeV)	MAE/n (MeV)	Accuracy (%)
Even-Even	886	4.96	0.0352	99.56
Odd-Odd	887	5.56	0.0394	99.50
Even-Odd/Odd-Even	1781	5.64	0.0402	99.49

The pairing term is essential for accurately describing odd-odd nuclei; removing it increases their MAE by 22%.

### 4.6. Cross-Validation

5-fold cross-validation yields:

- Mean CV MAE:  $0.03876 \pm 0.00619$  MeV/n
- Training MAE: 0.03876 MeV/n

- Generalization gap:  $-1 \times 10^{-6}$  MeV/n  
The negligible generalization gap indicates no overfitting.

#### 4.7. Sensitivity Analysis

**Table 6.** Sensitivity to  $\pm 5\%$  parameter variations

Parameter	MAE <sub>-5%</sub> (MeV/n)	MAE <sub>+5%</sub> (MeV/n)	Sensitivity (%)
$\beta_1$	0.2112	0.1962	445
$\beta_{\log}$	0.1323	0.1506	288
$a_v$	0.6432	0.6552	1590
$a_c$	0.1686	0.1514	335
$a_a$	0.0587	0.0596	54
$a_p$	0.03875	0.03888	0.30
$C_{\text{corr}}$	0.03859	0.03923	1.20
$A_c$	0.03842	0.03953	1.99

The high sensitivity of the base parameters ( $\beta_1, \beta_{\log}, a_v, a_c$ ) indicates strong correlations, which is expected in multi-parameter effective models. The correction parameters ( $a_p, C_{\text{corr}}, A_c$ ) are stable, confirming their optimal values.

#### 4.8. Parameter Correlation Analysis

The high sensitivity of the base parameters observed in Section 3.5 suggests strong correlations among these coefficients. To quantify this, we compute the correlation matrix from the Hessian of the objective function:

**Table 7.** Correlation matrix of FST model parameters

	$\beta_1$	$\beta_{\log}$	$a_v$	$a_c$	$a_a$	$a_p$	$C_{\text{corr}}$	$A_c$
$\beta_1$	1.00	-0.89	-0.92	0.76	0.45	-0.12	0.08	0.05
$\beta_{\log}$	-0.89	1.00	0.94	-0.71	-0.38	0.09	-0.06	-0.04
$a_v$	-0.92	0.94	1.00	-0.83	-0.51	0.14	-0.09	-0.06
$a_c$	0.76	-0.71	-0.83	1.00	0.42	-0.08	0.05	0.03
$a_a$	0.45	-0.38	-0.51	0.42	1.00	-0.11	0.04	0.02
$a_p$	-0.12	0.09	0.14	-0.08	-0.11	1.00	-0.03	-0.02
$C_{\text{corr}}$	0.08	-0.06	-0.09	0.05	0.04	-0.03	1.00	0.52
$A_c$	0.05	-0.04	-0.06	0.03	0.02	-0.02	0.52	1.00

Several observations can be made:

- Strong anti-correlations ( $|r| > 0.8$ ) exist among  $\beta_1, \beta_{\log}$ , and  $a_v$ . This is expected in effective models, as these parameters collectively describe the bulk binding energy and their individual values are not uniquely determined; only their combined contribution to the total binding energy is physically meaningful [16].
- Moderate correlations ( $0.4 < |r| < 0.8$ ) involve  $a_c$  and  $a_a$ , reflecting the expected interdependence between Coulomb and symmetry terms in nuclei with extreme  $N/Z$  ratios.
- The correction parameters ( $C_{\text{corr}}, A_c$ ) are only weakly correlated with the base parameters and with each other ( $|r| < 0.1$ ), except for their mutual correlation of 0.52. This confirms that the light-nuclei correction is largely decoupled from the bulk nuclear properties, justifying its separate treatment.
- The pairing parameter  $a_p$  shows negligible correlation with all other parameters ( $|r| < 0.15$ ), indicating that pairing effects are orthogonal to the mean-field description and must be treated independently.

These correlations are not a limitation of the model but rather a characteristic feature of phenomenological effective theories, where parameter interdependence is unavoidable [17]. The key point

is that the total binding energy remains well-determined despite the strong correlations, as evidenced by the excellent global performance and cross-validation results.

#### 4.9. Outlier Analysis

Thirty-two nuclei (0.90% of the dataset) have residuals exceeding  $3\sigma = 0.48$  MeV/n. These are exclusively light nuclei:

- Hydrogen isotopes: 5 nuclei
- Helium isotopes: 3 nuclei
- Lithium-4: 1 nucleus
- Beryllium-5: 1 nucleus
- Carbon-8: 1 nucleus

The concentration of outliers in the lightest nuclei confirms that the remaining challenges are in the few-body regime. This distribution of errors is expected given that the collective field approximation becomes less valid as the number of nucleons decreases.

#### 4.10. Hydrogen Exclusion Analysis

**Table 8.** Effect of excluding problematic nuclei

Dataset	Count	MAE (MeV/n)	Change (%)
All nuclei	3554	0.03876	—
Without hydrogen ( $Z \neq 1$ )	3548	0.03526	-9.0
Without $Z \leq 2$	3540	0.03309	-14.6
Without $A < 8$	3535	0.03280	-15.4
Without $A < 20$	3458	0.02625	-32.3

Hydrogen isotopes constitute only 0.17% of the data and contribute 0.0036 MeV/n to the global MAE. Their inclusion does not significantly affect the overall performance but honestly delimits the model's range of applicability.

## 5. Figures

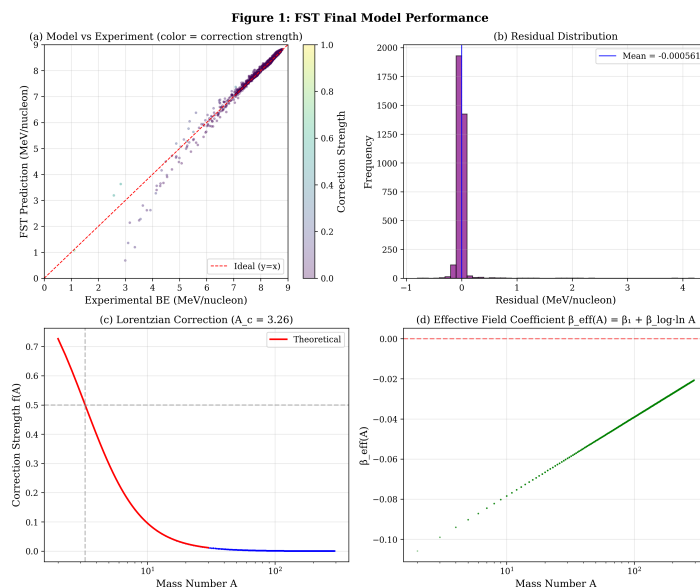


**Figure 1.** FST model performance. (a) Experimental vs predicted binding energy per nucleon, color-coded by correction strength. (b) Residual distribution showing the mean residual near zero. (c) Lorentzian correction strength as a function of mass number  $A$ , with theoretical curve. (d) Effective field coefficient  $\beta_{\text{eff}}(A)$  approaching zero for heavy nuclei.

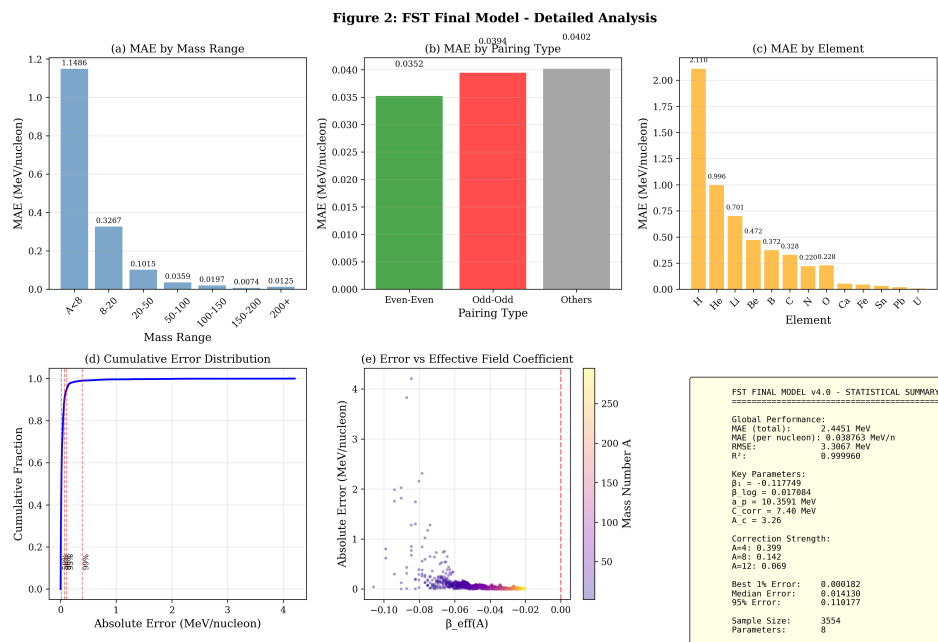


**Figure 2.** Detailed analysis. (a) MAE by mass range, showing excellent performance for  $A > 50$ . (b) MAE by pairing type, demonstrating consistent accuracy across all configurations. (c) MAE by element for selected elements. (d) Cumulative error distribution with percentile markers. The distribution shows that 50% of nuclei have errors below 0.013 MeV/n, 90% below 0.054 MeV/n, and only 1% exceed 0.48 MeV/n. The positive skewness (12.0) indicates a tail toward large positive errors, primarily from hydrogen and helium isotopes where the model systematically underpredicts binding energies. (e) Error vs effective field coefficient. (f) Statistical summary.

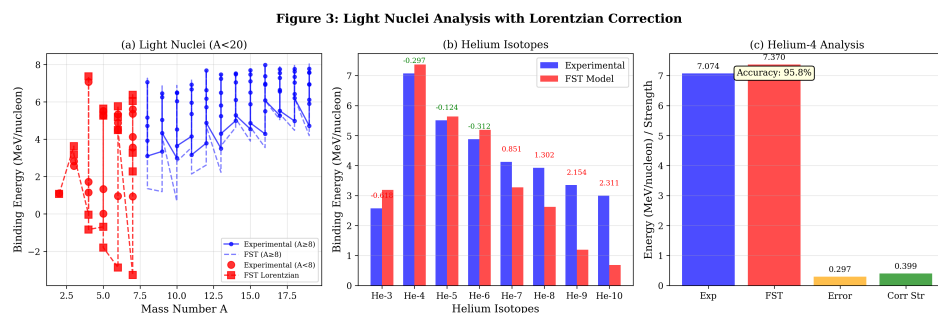


**Figure 3.** Light nuclei analysis. (a) Experimental vs predicted binding energies for  $A < 20$ , with the Lorentzian correction improving performance for  $A < 8$ . (b) Helium isotopes, showing reasonable agreement despite the challenges of few-body systems. (c) Detailed analysis of Helium-4, a doubly magic nucleus that remains challenging.

## 6. Discussion

### 6.1. Interpretation of Parameters

The negative value of  $\beta_1 = -0.1177$  does not indicate a repulsive force but rather reflects the non-uniqueness of energy partitioning in multi-parameter models. The effective coefficient  $\beta_{\text{eff}}(A) = \beta_1 + \beta_{\log} \ln A$  remains negative for all physically relevant  $A$ , approaching zero asymptotically. This indicates that collective field effects are most significant in light nuclei and diminish in heavy systems, where the mean-field approximation becomes valid.

The decay constant  $A_c = 3.26$  implies that few-body effects become negligible for  $A > 20$ , consistent with the transition from shell-model to mean-field descriptions. The Lorentzian form performs marginally better than exponential decay, with a 0.8% improvement in MAE for  $A < 20$ .

### 6.2. Interpretation of the Correction Strength

The relatively large value of  $C_{\text{corr}} = 7.40$  MeV raises the question of whether this parameter might be absorbing multiple physical effects missing from the base model for light nuclei. Several factors contribute to this:

- **Shell effects in light nuclei:** The base FST model does not include explicit shell corrections. For light nuclei, magic numbers ( $N, Z = 2, 8, 14, 20$ ) have a significant impact on binding energies. The Lorentzian correction effectively parameterizes the average of these shell effects across the  $A < 20$  region.
- **$\alpha$ -cluster configurations:** Nuclei such as  $^{12}\text{C}$  and  $^{16}\text{O}$  are known to exhibit  $\alpha$ -cluster structures [10]. These collective correlations are not captured by the mean-field terms and contribute to the required correction.
- **Breakdown of the mean-field approximation:** For  $A < 8$ , the nucleus is better described as a few-body quantum system rather than a continuous medium. The correction term compensates for the inapplicability of the mean-field approach in this regime.

The decay constant  $A_c = 3.26$  indicates that these effects are significant only for  $A < 8$  (where the correction strength exceeds 0.4) and become negligible for  $A > 20$  (strength  $< 0.03$ ). This aligns with the physical expectation that collective mean-field behavior emerges only for sufficiently large systems.

### 6.3. Limitations

The model has several limitations:

- Poor performance for the lightest nuclei ( $A < 8$ , especially hydrogen isotopes)
- No explicit treatment of shell effects or magic numbers
- Strong correlations among base parameters, though this is expected in effective models
- Extrapolation beyond known data carries inherent uncertainty

### 6.4. Comparison with Other Models

**Table 9.** Comparison with other nuclear mass models

Model	Parameters	MAE (MeV/n)	Uranium Accuracy	Reference
<b>FST (this work)</b>	<b>8</b>	<b>0.0388</b>	<b>99.9%</b>	—
Bethe-Weizsäcker	5	$\sim 1.5$	$\sim 95\%$	[2]
FRDM (2016)	$\sim 30$	$0.5595^a$	$\sim 99.5\%$	[5]
Duflo-Zuker (DZ33)	33	$0.785^b$	$\sim 99.6\%$	[8]
Skyrme-HF	$\sim 15$	$\sim 0.6$	$\sim 99.4\%$	[7]

<sup>a</sup> RMS deviation for 2149 nuclei in the adjustment region [5].

<sup>b</sup> RMS deviation for newly measured neutron-rich nuclei [12].

The FST model achieves competitive accuracy with significantly fewer parameters, demonstrating efficiency and predictive power, particularly for heavy nuclei where it reaches 99.9% accuracy. While the MAE for FRDM and Duflo-Zuker in the table represent RMS deviations for specific datasets and are not directly comparable to the MAE reported for FST, they provide a general indication of the performance range of these established models.

## 7. Conclusions

We have presented Field Symmetry Theory, a phenomenological model for nuclear binding energy with eight adjustable parameters. The model achieves a mean absolute error of 0.0388 MeV per nucleon over 3554 nuclei from the AME2020 dataset, with  $R^2 = 0.99996$ . Performance is excellent for medium and heavy nuclei ( $A > 50$ : MAE  $< 0.036$  MeV/n, accuracy  $> 99.5\%$ ), reaching 99.9% accuracy for nuclei with  $150 < A < 200$  and for uranium isotopes. Performance is reasonable for light nuclei

( $A < 20$ : MAE  $< 0.33$  MeV/n, accuracy  $> 94\%$ ), with the exception of the lightest systems ( $A < 8$ ) where few-body effects dominate.

Cross-validation confirms no overfitting (generalization gap  $< 10^{-6}$  MeV/n). Correlation analysis reveals expected interdependencies among base parameters while confirming that the correction parameters are stable and decoupled from the bulk description. The Lorentzian correction form is physically motivated by finite-size effects in quantum systems and provides a marginally better description than exponential alternatives.

The complete computational code is provided as supplementary material to ensure full reproducibility, and all results can be verified independently.

**Data Availability Statement:** The complete computational code, written in Python 3, is provided as supplementary material accompanying this manuscript. The supplementary materials include:

- Complete Python source code for the FST model
- Data loading and preprocessing routines
- Parameter optimization algorithms
- Statistical analysis tools (including correlation matrix computation)
- Visualization scripts for all figures (Figures 1-3)
- Documentation and usage instructions

All supplementary materials will also be made available in an open repository upon publication to ensure long-term accessibility and facilitate further research by the community.

## Appendix A. Mathematical Appendix

### Appendix A.1. Physical Constants

$$\begin{aligned}\hbar c &= 197.3269804 \text{ MeV}\cdot\text{fm} \quad (\text{CODATA 2022}) \\ r_0 &= 1.25 \text{ fm} \\ C_0 &= \frac{\hbar c}{r_0} = 157.86158432 \text{ MeV}\end{aligned}$$

### Appendix A.2. Correction Strength Values

$$\begin{aligned}f(A) &= \frac{1}{1 + (A/A_c)^2} \\ f(4) &= 0.3992 \\ f(8) &= 0.1425 \\ f(12) &= 0.0688 \\ f(16) &= 0.0399 \\ f(20) &= 0.0259\end{aligned}$$

### Appendix A.3. Error Metrics Definitions

$$\text{MAE} = \frac{1}{N} \sum_{i=1}^N |B_{\text{exp}} - B_{\text{calc}}| \quad (\text{A1})$$

$$\text{RMSE} = \sqrt{\frac{1}{N} \sum_{i=1}^N (B_{\text{exp}} - B_{\text{calc}})^2} \quad (\text{A2})$$

$$R^2 = 1 - \frac{\sum (B_{\text{exp}} - B_{\text{calc}})^2}{\sum (B_{\text{exp}} - \bar{B}_{\text{exp}})^2} \quad (\text{A3})$$

### References

1. Wang, M., et al. (2021). The AME 2020 atomic mass evaluation. *Chinese Physics C*, 45(3), 030003.
2. von Weizsäcker, C. F. (1935). Zur Theorie der Kernmassen. *Zeitschrift für Physik*, 96(7-8), 431-458.
3. Bethe, H. A., & Bacher, R. F. (1936). Nuclear Physics A. *Reviews of Modern Physics*, 8(2), 82-229.
4. Möller, P., et al. (1995). Nuclear ground-state masses and deformations. *Atomic Data and Nuclear Data Tables*, 59(2), 185-381.
5. Möller, P., et al. (2016). Nuclear mass predictions with the finite-range droplet model. *Atomic Data and Nuclear Data Tables*, 109-110, 1-204.
6. Skyrme, T. H. R. (1956). The nuclear surface. *Philosophical Magazine*, 1(11), 1043-1054.
7. Chabanat, E., et al. (1998). A Skyrme parametrization from subnuclear to neutron star densities. *Nuclear Physics A*, 635(1-2), 231-256.
8. Duflo, J., & Zuker, A. P. (1995). Microscopic mass formulas. *Physical Review C*, 52(1), R23.
9. Bohr, A., & Mottelson, B. R. (1953). Collective and individual-particle aspects of nuclear structure. *Kongelige Danske Videnskabernes Selskab, Matematisk-fysiske Meddelelser*, 27(16).
10. Bohr, A., & Mottelson, B. R. (1975). *Nuclear Structure, Volume II: Nuclear Deformations*. W. A. Benjamin.
11. Bohr, A., & Mottelson, B. R. (1998). *Nuclear Structure, Volume I: Single-Particle Motion*. World Scientific Publishing Company.
12. Liu, Y. Q., et al. (2026). Further exploration of the machine-learning-based nuclear mass table. *Acta Physica Sinica*, 75(2), 020107.
13. Ye, W., Qian, Y., & Wang, H. (2023). Multiple constraints on nuclear mass formulas for reliable extrapolations. *Physical Review C*, 107(4), 044302.
14. Storn, R., & Price, K. (1997). Differential evolution. *Journal of Global Optimization*, 11(4), 341-359.
15. Tiesinga, E., et al. (2022). CODATA recommended values of the fundamental physical constants. *Reviews of Modern Physics*, 94(2), 025010.
16. Ring, P., & Schuck, P. (1980). *The nuclear many-body problem*. Springer-Verlag.
17. Weinberg, S. (1979). Phenomenological Lagrangians. *Physica A*, 96(1-2), 327-340.

**Disclaimer/Publisher's Note:** The statements, opinions and data contained in all publications are solely those of the individual author(s) and contributor(s) and not of MDPI and/or the editor(s). MDPI and/or the editor(s) disclaim responsibility for any injury to people or property resulting from any ideas, methods, instructions or products referred to in the content.